



TL, OSL and ESR properties of nanostructured $\text{KAlSi}_3\text{O}_8\text{:Mn}$ Glass

E.L. Pires^a, S.H. Tatum^{a,b,*}, J.C.R. Mittani^b, A. Kinoshita^{c,d}, O. Baffa^d, L.V.E. Caldas^e

^aEscola Politécnica, Universidade de São Paulo, Brazil

^bFaculdade de Tecnologia de São Paulo, CEETEPS, Praça Cel.Fernando Prestes, 30, 01124-060 São Paulo, Brazil

^cUniversidade Sagrado Coração, Ribeirão Preto, Brazil

^dFaculdade de Filosofia, Ciências e Letras de Ribeirão Preto, Universidade de São Paulo, Brazil

^eInstituto de Pesquisas Energéticas e Nucleares, IPEN/CNEN-SP, Brazil

ARTICLE INFO

Article history:

Received 17 November 2010

Received in revised form

28 March 2011

Accepted 29 April 2011

Keywords:

Thermoluminescence

OSL

ESR

Silicate glasses

Environmental dosimetry

Nanoparticles

ABSTRACT

Glass samples of $\text{KAlSi}_3\text{O}_8\text{:Mn}$ were synthesized by sol-gel technique and the incorporation effects of Mn on the TL, OSL and ESR signals were studied. Its morphologies were analyzed through Transmission Electron Microscopy (TEM), Energy Dispersive Spectroscopy (EDS). Samples were obtained with five different molar concentrations of 0.25, 0.5, 1, 2 and 5 mol% of Mn. TEM micrographs indicated the occurrence of nanoparticles of Mn_2SiO_4 with 200 nm of size approximately. Results of TL spectra showed a broad emission band from 450 to 700 nm with a peak at 575 nm approximately, and fitting very well with the characteristic lines of the Mn^{2+} emission features. The OSL decay can be fitted by a sum of two exponentials. A proportional dose response curves of the OSL and TL for samples irradiated with γ -rays were verified. ESR results supplied six lines related to Mn^{2+} ions are observed superposed by a large isotropic line; the Hamiltonian components of these lines determined through simulation are $I = 5/2$, $s = 5/2$, $g = 2.0060$, $A = 8.3$ mT and $s = 1/2$, $g = 2.0007$ for the Mn^{2+} and isotropic lines.

© 2011 Elsevier Ltd. All rights reserved.

1. Introduction

For luminescence dating purposes, an evaluation of the dose-rate of a specific sampling site should be made in order to obtain the age of the sample. Contributions of gamma, beta, alpha and cosmic rays to the annual dose are determined by several techniques, such as: neutron activation, gamma-spectroscopy, X-ray fluorescence, inductively coupled plasma mass spectrometry (ICPMS); all have advantages and disadvantages, and they are expensive techniques.

In the case of a reliable assessment of the gamma contribution, the measurement should be made in uniform soil surroundings the sample, forming a sphere with 0.3 m of radius, which is the value of the range of gamma photons with energy about 2 MeV in the soil. The cosmic ray contribution is small, about 150 $\mu\text{Gy/a}$ at ground level, and has a rapid fall off in the first 30 cm depth, the value being reduced to half at 5 m depth. The on-site methods such as thermoluminescence dosimetry (TLD) capsules and gamma-spectroscopy automatically include the cosmic ray contribution.

The inhomogenities effects of beta particles, originating from potassium and rubidium found in K-feldspar grains are observed in

some cases and this contribution can be well evaluated with the use of specific TLD capsules. Two TLD phosphors are commonly used in dating: natural calcium fluoride (fluorite) and the $\text{CaSO}_4\text{:Dy}$. Both are used because their effective atomic numbers are close to the quartz one (11.75).

Therefore, the use of TLD and OSL dosimeters for dose-rate measurements seems highly appropriate and attractive, taking into account their low cost. Much effort has been made in order to find new materials and techniques to obtain accurate doses, mainly in the radiobiological applications where the dosimetric material has to be tissue-equivalent. The main objective of this work is to propose a new material composed by $\text{KAlSi}_3\text{O}_8\text{:Mn}$. ESR, TL, OSL measurements and, as well as, TL emission spectra of the materials will be presented.

2. Materials and methodology

Glass samples of KAlSi_3O_8 were obtained with five different concentrations 0.25, 0.5, 1, 2 and 5 mol% of Mn. The sol-gel technique was used for the synthesis with stoichiometric amounts of: aluminium tri-sec-butoxide (ATSB), tetraethyl-orthosilicate (TEOS) and potassium hydroxide (KOH). The Mn was added as a carbonate compound.

The morphological characteristics of the samples were analyzed using a Philips CM200 Transmission Electron Microscopy (TEM)

* Corresponding author. Faculdade de Tecnologia de São Paulo, CEETEPS, Praça Cel.Fernando Prestes, 30, 01124-060 São Paulo, Brazil. Fax: +55 11 33267611.

E-mail address: tatum@fatecsp.br (S.H. Tatum).

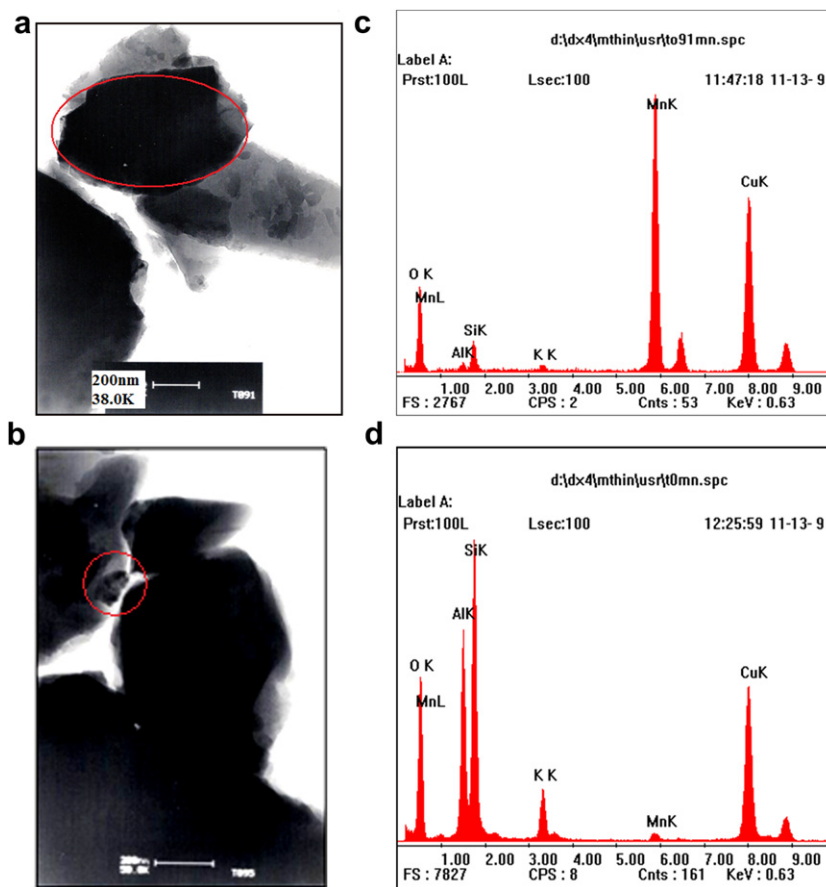


Fig. 1. a) TEM image of 5 mol% Mn doped KAlSi_3O_8 glass, with Mn_2SiO_4 nanoparticle with size about 700 nm; b) TEM image of 5 mol% Mn doped KAlSi_3O_8 glass, with Mn_2SiO_4 nanoparticle with size about 100 nm; c) EDS results for sample a), showing high Mn concentration and d) EDS results for sample b) with low Mn concentration.

equipped with Energy dispersive spectroscopy (EDS) operating at 160 keV. The TL and OSL measurements were carried out in a TL/OSL 1100-series reader from Daybreak Nuclear and Medical Systems Inc. TL measurements were obtained for visible region with a Schott BG-39 (340–610 nm) and for UV region with Schott U-340 optical filter. The heating rate used in all the TL measurements was 10 °C/s. The OSL measurements were taken using an array of blue (470 nm) LEDs for sample excitation and the Schott U-340 optical filter in front of the PMT for detection. The γ -irradiations were performed at RT with a ^{60}Co source with dose-rate of 28.7 Gy/h.

All ESR spectra were taken at RT, below micro-wave power saturation, by means of the homodyne X-band JEOL FA-200 spectrometer. Experimental parameters were: micro-wave power of 10 mW, modulation width 0.1 mT, modulation frequency 100 kHz and scan range 150 mT. The software Simfonia (Bruker) was employed for spectra simulation. TL spectrum of the sample was obtained with a Varian 500 Cary Eclipse Fluorescence Spectrometer which was coupled to the TL/OSL reader by a waveguide.

3. Results and discussion

In order to investigate the morphology of the obtained samples and the effects of Mn doping, TEM images were made. Fig. 1a and b show TEM image for sample doped with 5 mol% of Mn. The predominance of vitreous structure together with Mn_2SiO_4 nanoparticles were identified by electron beams diffraction, with size ranging from 100 to 700 nm approximately. The Mn presence in the

samples is confirmed by EDS results, which is showed in Fig. 1c and d. The undoped sample did not show Mn peak, and the occurrence of Cu, in all the measurements, was due to sample holder contamination.

Fig. 2a shows typical ESR spectra for samples with 0.25, 0.5, 1, 2 and 5 mol% of Mn. The six lines related to Mn^{2+} ions are observed superposed by a large isotropic line. The Hamiltonian components of these lines determined through simulation are $I = 5/2$, $s = 5/2$, $g = 2.0060$, $A = 8.3$ mT and $s = 1/2$, $g = 2.0007$ for the Mn^{2+} and isotropic lines, respectively, and are shown in Fig. 2b. Mn^{2+} magnetically diluted should show a sextet but when inter-ion interaction occurs a broad line start to appear. This is clearly seen in Fig. 2a; a small percentage as 0.5% gives rise to a broad ESR line. This indicates that probably Mn^{2+} is agglomerated in some regions of the glass leading to an inter-ion interaction (Borse et al., 1999; Silva et al., 2009). This result is in agreement with the luminescence results that show a decrease in intensity for higher Mn^{2+} concentrations.

The Mn doping greatly improved the TL emission of the dosimetric peak at 180 °C (Fig. 3a). The peak temperature value seems to be related to the matrix elements, because it is different to those found in $\text{CaSO}_4:\text{Mn}$, and $\text{CaF}_2:\text{Mn}$, which appears at 80 and 250 °C, respectively (McKeever, 1985), the first sample despite being highly sensitive cannot be used due to its low peak temperature. Dotzler et al. (2007) observed several TL peaks emitted by synthesized $\text{RbMgF}_3:\text{Mn}$, previously irradiated with X-rays. The sample doped with 0.5 mol% Mn yielded the best TL response, while an increase in Mn concentration causes a decrease in TL response due to concentration quenching. No results about concentration quenching of Mn

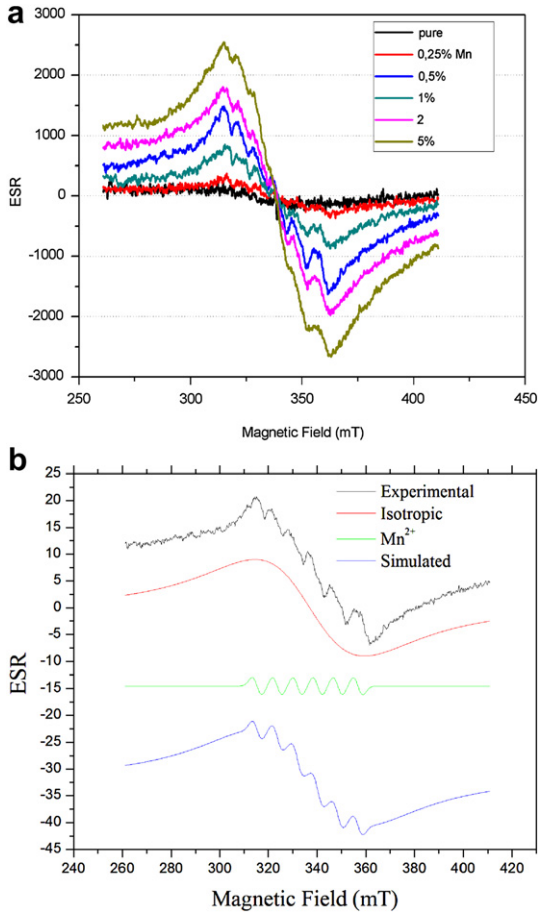


Fig. 2. a) X-band ESR spectrum of irradiated KAlSi₃O₈: Mn glass, with different Mn concentrations and b) From top to bottom, ESR spectra of original, deconvoluted and simulated signals, showing the good agreement between the simulated and experimental signal.

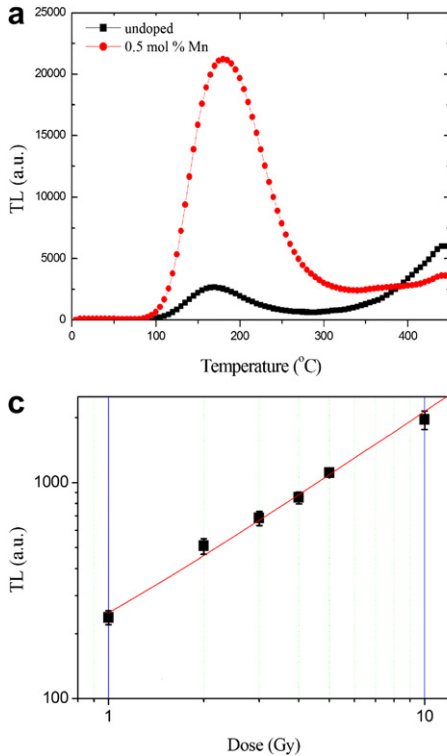


Fig. 3. a) TL glow curves of KAlSi₃O₈ glass, black square indicated undoped sample and red circles indicated 0.5 mol % of Mn sample, irradiated with a dose of 10 Gy; b) TL spectra of 0.5 mol % Mn doped KAlSi₃O₈ glass and TL growth curve of 0.5 mol % Mn doped KAlSi₃O₈ glass, the sample was irradiated with a dose of 188 kGy and c) TL growth curve of the 0.5 mol % of Mn sample. (For interpretation of the references to colour in this figure legend, the reader is referred to the web version of this article.)

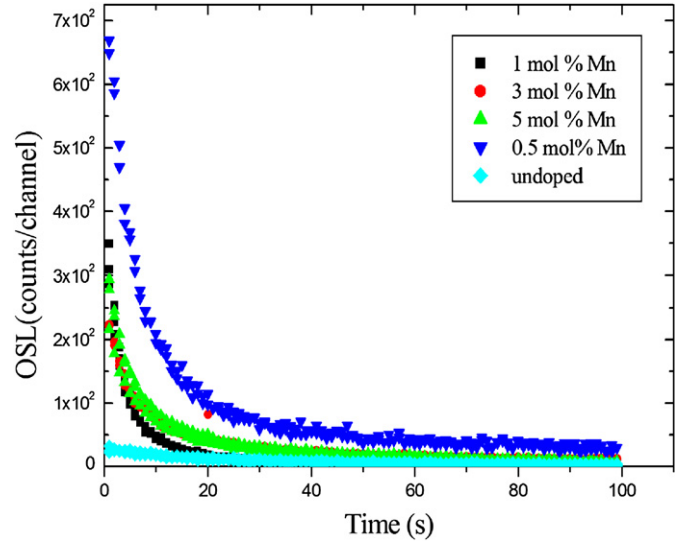


Fig. 4. OSL decay curves, in UV region, of undoped and 0.25, 0.5, 1, 2 and 5 mol% Mn doped KAlSi₃O₈ samples, obtained with blue excitation. (For interpretation of the references to colour in this figure legend, the reader is referred to the web version of this article.)

for TL were found in the literature; however, several authors obtained values between 0.07 and 4% of Mn, for photoluminescence results in ZnS (Khosravi et al., 1995; Murugadoss et al., 2010), on this way the value of 0.5 mol% obtained in the present work is in agreement with them. The concentration quenching phenomenon can be attributed due to the migration of the excitation energy between Mn²⁺ ions pairs; the excitation energy is transferred from one Mn²⁺ to its adjacent Mn²⁺ by non radiative transition, until to a quenching defect state.

The TL spectrum of this sample presents a broad emission band from 450 to 700 nm with a peak at 575 nm approximately (Fig. 3b).

Usually this emission band is related to the ${}^4T_{1g} \rightarrow {}^6A_{1g}$ transition level of the Mn^{2+} , considering an O_h crystal field symmetry. Therefore, our results indicate that Mn^{2+} ions are presented in different environments produced by $KAlSi_3O_8$ glasses, which results in blue and orange luminescence. Murugadoss et al. (2010) observed the ZnS:Mn photoluminescence and they concluded that when the Mn^{2+} is incorporated into the ZnS lattice, it leads to orange emission, and for high Mn concentration the quenching of blue band is observed, and the emission in the yellow–orange region takes place predominantly. The Mn^{2+} emission at 560 nm was observed in natural feldspar crystals too (Garcia-Guinea et al., 1996; Prescott and Fox, 1993). In the present case, there are formations of Mn_2SiO_4 nanoparticles emitting in the blue/orange region and for high Mn concentration a decrease in all bands was noted. The TL growth curve was almost proportional with the doses from 1 to 10 Gy, as can be seen in Fig. 3c.

A very high intensity signal with a fast OSL decay signal was obtained with 0.5% Mn doped sample, it is about 20 times higher than the OSL signal supplied by undoped one (Fig. 4). A proportional dose response of the OSL signal was verified for samples irradiated with γ -radiation, however the response with the dose is not intense as TL one. Similar result about anti-Stokes OSL emission in the ultraviolet region, of Mn doped sample, has not been reported yet in the literature, only phosphors presenting Stokes emission, as the Henke et al. (2007) work; they showed results of OSL emission at 560 nm of $RbCdF_3:Mn$ excited with a laser diode at 375 nm.

4. Conclusions

The $KAlSi_3O_8$ matrix was favourable to the production of Mn^{2+} centres observed by the ESR measurements, using the sol-gel process the formation of Mn_2SiO_4 nanoparticles was observed inside the glass. The Mn incorporation increased the efficiency of TL and OSL responses of the matrix; these nanoparticles have a size of 200 nm approximately. The concentration of 0.5 mol% Mn was found to be the best value for the luminescent response enhancement.

Blue and orange TL emission related to Mn^{2+} were observed; probably the TL emission mechanism can be explained due to the recombination of Mn^{3+} centre with an electron in the heating process. During the TL measurements, the Mn^{2+} in excited state is

created and TL is emitted subsequently due to Mn^{2+} relaxation in to fundamental state. The Mn^{3+} is created previously by irradiation with ionizing radiation; this assumption was consistent with Dotzler et al. (2007) work. In the samples with low TL response, the Mn ions, probably, have with different valence numbers.

The anti-Stokes emission was observed in the OSL measurements, where the UV emission was produced under blue excitation. An OSL proportional dose response was obtained for gamma radiation.

The effective atomic number of $KAlSi_3O_8:Mn$ is about 13.36, similar to feldspar (13.33) and quartz (11.75), carbonates (15.63) sediments, therefore, these sample can be used in environmental dosimetry and maybe very useful for the TL and OSL dating area.

Acknowledgements

Partial financial support from the Brazilian agencies FAPESP, CAPES and CNPq is thankfully acknowledged.

References

- Borse, P.H., Shrinivas, D., Shinde, R.F., Date, S.K., Vogel, W., Kulkarni, S.K., 1999. Effect of Mn^{2+} concentration in ZnS nanoparticles on photoluminescence and electron-spin resonance spectra. *Phys. Rev. B* 60 (12), 8659–8664.
- Dotzler, C.J., Williams, G.V.M., Edgar, A., 2007. Thermoluminescence, photoluminescence and optically stimulated luminescence properties of X-ray irradiated $RbMgF_3:Mn^{2+}$. *Phys. Stat. Sol. (c)* 4 (3), 992–995.
- Garcia-Guinea, J., Rendell, H.M., Sanchez-Muñoz, L., 1996. Luminescence Spectra of Alkali Feldspars: Some Relationships between Structural Features and Luminescence Emission.
- Henke, B., Rogulis, U., Schweizer, S., 2007. Optical and electron paramagnetic resonance studies on radiation defects in Mn-activated $RbCdF_3$. *Phys. Stat. Sol. (c)* 4 (3), 1071–1074.
- Khosravi, A.A., Kundu, M., Kuruvilla, B.A., Shekhawat, G.S., Gupta, R.P., Sharma, K.A., Vyas, P.D., Kulkarni, S.K., 1995. Manganese doped zinc sulphide nanoparticles by aqueous method. *Appl. Phys. Lett.* 67, 2506–2508.
- McKeever, S.W.S., 1985. *Thermoluminescence of Solids*. Cambridge University Press, USA.
- Murugadoss, G., Rajamannan, B., Ramasamy, V., 2010. Synthesis, characterization and optical properties of water-soluble ZnS: Mn^{2+} nanoparticles. *J. Lumin.* 130, 2032–2039.
- Prescott, J.R., Fox, P.J., 1993. Three-dimensional thermoluminescence spectra of feldspar. *J. Phys. D Appl. Phys.* 26, 2245–2254.
- Silva, R.S., Morais, P.C., Sullasi, H.S.L., Ayta, W.E.F., Qu, F., Dantas, N.O., 2009. Magnetic and optical characterization of Mn-doped PbS nanocrystals supported in oxide glass matrix. *J. Alloys Compd.* 483, 204–206.